Effect of electrode flux composition on impact toughness of austenitic stainless-steel weld metal

by G. Lubbe[1], P.G.H. Pistorius[1], and D.S. Konadu[1,2]

*Paper written on project work carried out in partial fulfilment of BEng (Metallurgical Engineering) degree

Affiliation:
[1]Department of Materials Science and Metallurgical Engineering, University of Pretoria, Pretoria, South Africa.
[2]Department of Materials Science and Engineering, University of Ghana, Accra, Ghana.

Correspondence to:
P.G.H. Pistorius

Email:
pieter.pistorius@up.ac.za

Dates:
Received: 28 Oct. 2021
Revised: 12 Apr. 2022
Accepted: 12 Apr. 2022
Published: July 2022

How to cite:
Lubbe, G., Pistorius, P.G.H., and Konadu, D.S. 2022
Effect of electrode flux composition on impact toughness of austenitic stainless-steel weld metal.
Journal of the Southern African Institute of Mining and Metallurgy, vol. 122, no. 7, pp. 323–330

DOI ID:
http://dx.doi.org/10.17159/2411-9717/1879/2022

ORCID:
P.G.H. Pistorius
https://orcid.org/0000-0001-6582-8157

Synopsis

The aim of this investigation was to determine whether the composition of a shielded-metal arc-welding electrode coating affected the low-temperature impact toughness of austenitic stainless-steel weld metal. It is generally accepted that increases in the δ-ferrite and nitrogen contents result in a decrease in toughness at low temperatures. Weld metal from electrodes with a basic coating also generally exhibit better toughness than those from rutile (acidic) electrodes. An increase in basicity was expected to decrease the number and size of inclusions, which in turn provides a tougher weld metal. Three commonly available potassium–rutile E308L electrodes were used, complying with the E308L-16 and E308L-17 specifications. Analysis of the electrode coatings showed very similar chemistry and basicity. Significant differences in the inclusion contents of the weld metals were observed: the E308L-17 weld metal had a lower inclusion content (1.4% by volume) than the E308L-16 weld metal (3.7%). The former had higher impact toughness at all temperatures, despite a slightly higher nitrogen content. Regression analysis confirmed that the inclusion content had a significant effect on the impact toughness at all temperatures.

Keywords

Shielded-metal arc welding, inclusions, flux composition, austenitic stainless steel, ferrite number.

Introduction

Austenitic stainless steels are face-centred cubic Fe-Cr-Ni alloys that are widely used at low temperatures (among many other applications) due to the absence of a ductile-to-brittle transition, which is present in steels with a ferritic body-centred cubic structure (Hertzberg, 1995). Many austenitic stainless steel weld metals contain some δ-ferrite. Predictions of the amount of δ-ferrite (often expressed in terms of the ferrite number, FN) and the primary solidification mode can be made using the WRC-1992 diagram (Kotecki and Siewert, 1992). By calculating the chromium equivalent, which is the combined contributions of Cr, Mo, and Nb to ferrite formation, and the nickel equivalent, which is the combined contributions of Ni, C, N, and Cu to austenite stabilization, a prediction of FN can be made (Kotecki and Siewert, 1992). Electrode manufacturers typically guarantee a FN between 4 and 10, which indicates that the primary solidification mode will be ferritic. This decreases the probability of solidification cracking (Szumachowski and Reid, 1978).

Factors that affect the impact toughness of austenitic stainless steel at lower temperatures have been extensively explored (Kamiya, Kumagai, and Kikuchi, 1992; Lee and Dew-Hughes, 1982; Read *et al.*, 1980; Reed and Horiuchi, 1982; Szumachowski and Reid, 1978). One of the most critical factors affecting the toughness of austenitic stainless steel at low temperatures is the content and morphology of the δ-ferrite (Kamiya, Kumagai, and Kikuchi, 1992; Szumachowski and Reid, 1978). At higher impact testing temperatures, about 10% δ-ferrite resulted in the best impact toughness; however, at a testing temperature of –196°C, the presence of any δ-ferrite reduced the impact toughness (Lee and Dew-Hughes, 1982).

The effect of δ-ferrite on the impact toughness of austenitic stainless steel has been rationalized by classifying its morphology as globular, vermicular, or lacy. The presence of vermicular ferrite lowers impact toughness at lower temperatures to a greater extent than the other two forms, an effect attributed to vermicular δ-ferrite being parallel to the [100] plane, which is the preferential plane for cleavage fracture. Globular ferrite shows little to no brittle fracture because of low stress concentrations. Lacy ferrite shows little brittle fracture due to a Kurdjumov–Sachs relationship between the ferrite and

austenite phases. The most likely ferrite structure is vermicular, due to the low expected FN (Kamiya, Kumagai, and Kikuchi, 1992). A certain minimum amount of δ-ferrite is necessary to prevent solidification cracking in weld metal by ensuring the solidification of primary ferrite. Consequently, the weld metal becomes the critical part of a welded joint in low-temperature applications. Industrial focus concerning austenitic stainless steel applications at low temperatures is therefore mainly on the δ-ferrite content; other factors, such as the flux composition of the electrode coating or inclusion content of the weld metal, are paid little attention (Szumachowski and Reid, 1979).

Fluxes for shielded-metal arc-welding processes can be classified as rutile, basic-rutile, or basic. Constituents such as SiO_2, Al_2O_3, and TiO_2 that are present in acidic fluxes are oxide network-formers and generally increase the size and number of oxide inclusions in the weld metal compared with basic and neutral fluxes. Basic fluxes contain constituents such as CaO and MgO, which break the networks created by silica (Entrekin, 1979). The basicity index (BI) is calculated in terms of the mass percentages of the various components:

$$BI = \frac{CaO + CaF_2 + MgO + K_2O + Na_2O7 + Li_2O + 0.5(MnO + FeO)}{SiO_2 + 0.5(Al_2O_3 + TiO_2 + ZrO_2)} \quad [1]$$

A BI value of less than unity indicates an acidic flux, between unity and 1.2 is neutral, and above 1.2 is classified as basic (Entrekin, 1979). Researchers have noted that electrodes with a basic composition result in a weld metal with a higher impact toughness than that of rutile electrodes. For example, a linear regression model was used to predict that a basic electrode tested at –196°C would have 0.07 mm greater lateral expansion than weld metal of the same composition deposited with rutile electrodes. The associated difference in impact toughness was about 5 J (Szumachowski and Reid, 1978).

From the AWS specification governing austenitic stainless steel electrodes (AWS SFA-5.4, 2006), the suffix (-15, -16, or -17) refer to the usability of an electrode with a specific coating. The -15 electrode (not available in South Africa at the time of this investigation) has a basic coating and can be used using a direct current electrode-positive (DCEP) polarity in all positions. The coatings for -16 electrodes contain readily ionizable elements (potassium is mentioned specifically in the specification); these electrodes can be used with either DCEP or alternating current (AC) in all positions. The coating of the -17 electrodes was modified by replacing some of the titanium-rich oxides in the -16 coating with silica. Similar to -16 electrodes, -17 electrodes can be used in all positions, with DCEP or AC. In older versions of the AWS SFA-5.4 specification, -16 and -17 electrodes were classified as -16. The change in usability of the -17 electrodes, associated with a slower freezing slag, necessitated separation of the -16 and -17 electrode types. The specification does not define differences in chemical composition of either the electrode coating or of the weld deposit.

The aim of this investigation was to determine the effect of the inclusion content from varying flux compositions on the low-temperature impact toughness of austenitic stainless-steel weld metal, using commonly available electrodes.

Experimental procedure

AISI 304L austenitic stainless-steel plates, 200 mm long × 150 mm wide × 15 mm thick, were used to fabricate butt welds with double bevel edges with an included angle of 60°. The root opening was 3 mm, which is typical practice. A Lincoln Electric S350 power supply was used. A multipass weld was deposited in a horizontal flat welding position. The welding current varied between 100 and 140 A, closely following the limits set by the electrode manufacturers. The heat input and, as a consequence, the weld bead size was reasonably constant for the different weld beads in a specific weld bead, and between different butt welds. E308L electrodes with a diameter of 4 mm from three different suppliers were used. Electrodes A and B were of E308L-16 type and electrode C was E308L-17; the electrode type was as stated by the electrode manufacturer. Extracts from the data-sheets for these electrodes and comparisons of the important parameters are given in Table I. From the data supplied by the electrode manufacturers, electrode C was expected to produce a weld deposit with slightly higher impact toughness.

The flux was assayed by X-ray fluorescence and its basicity calculated using Equation [1]. Full-size Charpy impact test specimens were machined so that the notch was at the centreline of the butt weld and were tested according to the ASTM E2298-15 standard at a range of temperatures from room temperature to -196°C. The FN was determined according to AWS A4.2-98, using a Fischer MP3B Feritscope (Lippold and Kotecki, 2005). FN measurements were done on the top surface of the weld bead after light grinding. Ten FN measurements were performed on every weld bead. The weld metal chemical composition was determined on a cross-section of the welded joint by means of optical emission spectroscopy (OES). During OES analysis, care was taken to sample the weld beads, but not the base metal. The inclusion contents of the weld metals were measured in four different areas. Polished unetched sections of each weld bead were taken and nine micrographs of each sample were analysed at 100× magnification. The area fraction and sizes of the inclusions were measured using ImageJ optical analysis software. The microstructure was revealed by etching using 100 g/L oxalic acid. Additionally, polished sections of the weld metal were etched with standard *aqua regia* with a hydrochloric acid: nitric acid ratio of 3:1. Charpy impact fracture surfaces generated at –196°C and 20°C were examined by scanning electron microscopy.

Results

The flux composition and basicity index of the three electrodes are given in Table II. The BI values were similar and less than unity, indicating that all three had acidic coatings (Entrekin, 1979). It is likely that the behaviour of an electrode with a specific coating does not depend only on the basicity index but also on the constituents of the electrode coating and possibly the presence of trace elements in the electrode coating. In addition, comparison

Table I

Extracts from manufacturers' data-sheets for the electrodes used in this study

Electrode		A	B	C
Electrode type		E308L-16	E308L-16	E308L-17
FN		4-10	3-10	3-10
Impact toughness (J)	20°C	67	70	70
	-50°C	-	48	-
	-60°C	-	38	49
	-196°C	36	-	-

Table II

Flux compositions (mass%) obtained by XRF

Element	Reported as	Electrode A	Electrode B	Electrode C
Electrode type		E308L-16	E308L-16	E308L-17
C	C	1.42	1.19	1.23
S	S	0.028	0.026	0.016
Mn	MnO	1.34	1.71	1.72
P	P_2O_5	0.15	0.095	0.11
Si	SiO_2	24.8	21.8	20.5
Cr	Cr_2O_3	0.78	0.96	0.72
Ni	NiO	0.07	0.71	0.15
Cu	CuO	≤ 0.01	≤ 0.01	≤ 0.01
Al	Al_2O_3	5.17	4.34	4.17
V	V_2O_5	≤ 0.005	≤ 0.005	≤ 0.005
Ti	TiO_2	47.1	50.8	53.0
Co	CoO	0.047	0.058	0.056
Ca	CaO	9.09	7.10	8.15
Mg	MgO	≤ 0.005	0.064	0.23
Fe	FeO	6.38	7.32	6.07
K	K_2O	3.06	2.97	3.28
BI		0.31	0.30	0.32

of the flux composition of electrode C (the only -17 electrode in this study) showed a lower SiO2 and a higher TiO_2 content than electrodes A and B (which were -16 electrodes), contrary to the description in the relevant specification (AWS SFA-5.4, 2006). The reasons for this discrepancy between the flux composition and the stated electrode type were not clear, but could be related to a difference in usability, as determined by the electrode manufacturer, and not to the SiO_2 and TiO_2 content.

Table III gives the weld metal chemistry and predicted ferrite content (expressed as FN) of the three weld deposits. The weld metal from electrode B contained 0.84%Si, above the specified limit of 0.75%, and 20.4% Cr, marginally above the specified limit of 20%.

Table IV summarizes the most important results. Electrodes A and C showed similar weld metal FN values, at 5.2 and 4.9, respectively; that from electrode B had a significantly higher FN of 9.4. The predicted solidification mode in all three cases was primary ferrite solidification, which is associated with low risk of solidification cracking (Szumachowski and Reid, 1978). The inclusion contents from electrodes A and B were similar, at 3.8% and 3.7%, respectively. Electrode C resulted in a weld deposit with a much lower inclusion content of 1.4%. The impact toughness at –196°C in relation to that at ambient temperature (R_o/R_t) was lowest for electrode B, which had the highest FN. With increasing impact testing temperature, the average impact toughness values generally increased for all electrodes. With the exception of –196°C, all testing temperatures showed a gradual impact toughness increment from electrode A to electrode C. The exception was a high value of 39 J for electrode A, which decreased to 34 J for electrode B and then increased to 53 J for electrode C. Lateral expansion (LE) measurements showed similar trends to the average impact toughness values.

Figure 1 shows the results of the impact tests at different temperatures as well as those of Szumachowski and Reid 1979). The latter reported lower impact toughness than this investigation, but did show higher impact toughness at all temperatures for the basic electrodes (E308L-15) compared with the rutile electrodes (E308L-16). The results of this investigation showed higher impact toughness values for these low-basicity rutile electrodes than previously published. Significant differences in impact toughness between the three electrodes were also observed. Weld metal from electrode C had the highest impact toughness value at all tested temperatures. Lateral expansion of every Charpy impact test specimen, plotted as a function of impact energy, confirmed the consistency of the impact test results (Figure 2).

Figure 3 shows a typical weld metal microstructure. All three weld deposits showed a microstructure containing δ-ferrite with vermicular structure, which is associated with lower impact toughness values (Kamiya, Kumagai, and Kikuchi, 1992).

Table III

Weld metal chemical compositions (mass%) from the three electrodes. The FN, as predicted from the chemical composition, is also given

Element	Specification		Sample		
	Minimum	Maximum	Electrode A	Electrode B	Electrode C
C		0.03	0.019	0.021	0.021
Mn		2.0	0.66	0.76	0.75
S		0.03	0.010	≤ 0.005	≤ 0.005
P		0.045	0.033	0.023	0.018
Si		0.75	0.72	0.84	0.71
Cr	18	20	18.9	20.4	19.3
Mo			0.13	0.03	0.08
Ni	8	12	9.64	9.68	9.84
Cu			0.14	0.06	0.04
Al			≤ 0.005	≤ 0.005	≤ 0.005
V			0.068	0.059	0.060
Nb			≤ 0.005	0.012	0.012
Ti			0.007	0.010	0.009
Co			0.12	0.058	0.036
N			0.0661	0.0598	0.0810
Cr_{eq}			19.03	20.44	19.39
Ni_{eq}			11.99	11.93	12.61
Predicted FN			5	11	5

Table IV

Summary of results: actual ferrite number, volume fraction inclusions, impact energy (IE), and lateral expansion (LE) at a range of test temperatures, and change in impact toughness from 20°C to –196°C, expressed as R_o/R_t (R_o – impact toughness at –196°C; R_t – impact toughness at 20°C)

	Electrode A		Electrode B		Electrode C	
Measured FN	5.2 ± 0.6		9.4 ± 1.5		- 4.9 ± 0.4	
Volume fraction inclusions (%)	3.8		3.7		1.4	
Testing temperature (°C)	IE (J)	LE (mm)	IE (J)	LE (mm)	IE (J)	LE (mm)
-196	32	0.27	46	0.47	46	0.45
-196	46	0.59	22	0.22	60	0.60
-87	54	0.61	72	0.88	72	1.06
-87	54	0.83	60	0.60	62	0.80
-50	34	0.51	74	0.90	86	1.06
-50	60	0.97	82	1.22	74	1.09
0	64	1.08	84	1.23	104	1.46
20	80	1.29	94	1.12	106	1.76
R_0/R_r	0.49		0.36		0.50	

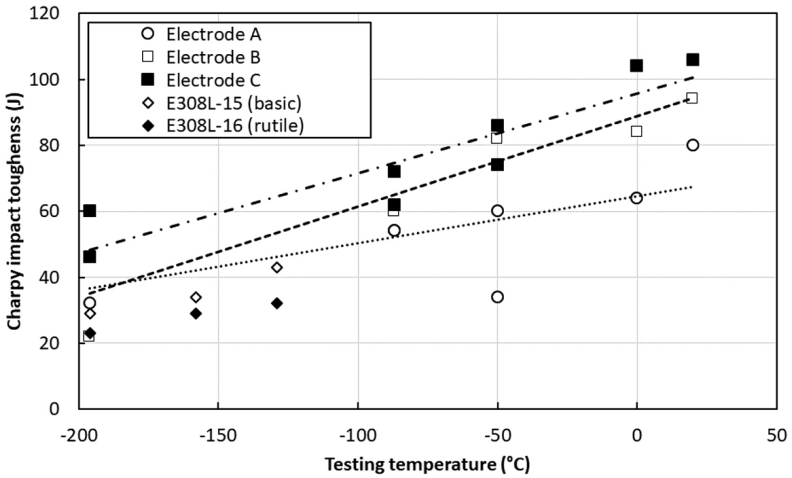

Figure 1—Comparison of measured impact toughness of three weld metals with published results for basic and rutile weld deposits (Szumachowski and Reid, 1978)

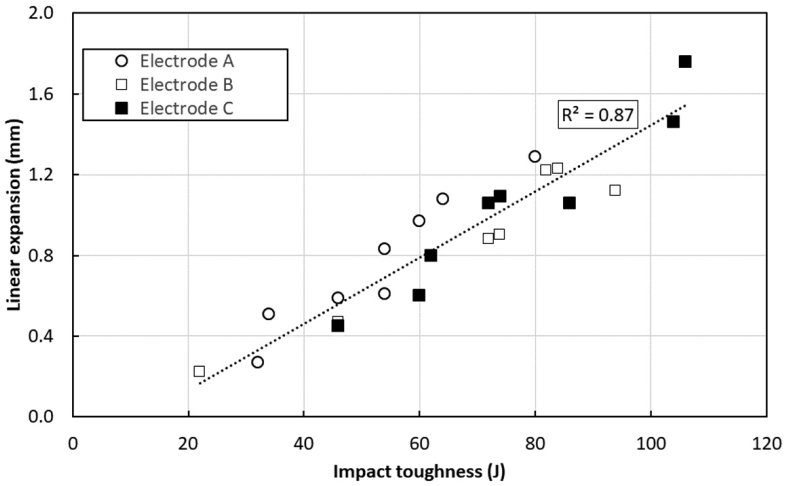

Figure 2—Lateral expansion as a function of impact energy, as a check on the consistency of the impact test results

Figure 4 shows fracture surfaces of the impact toughness coupons tested at –196°C. The fracture surfaces displayed micro-voids consistent with ductile fracture; limited cleavage fracture was observed. Typical of weld metal, inclusions were visible on all fracture surfaces. Many large broken inclusions were visible on the fracture surface of the weld metal from electrode A (Figure 4a).

Figure 5 shows the particle size distribution of the inclusions as a fraction of the inclusion content in the steel. Although the

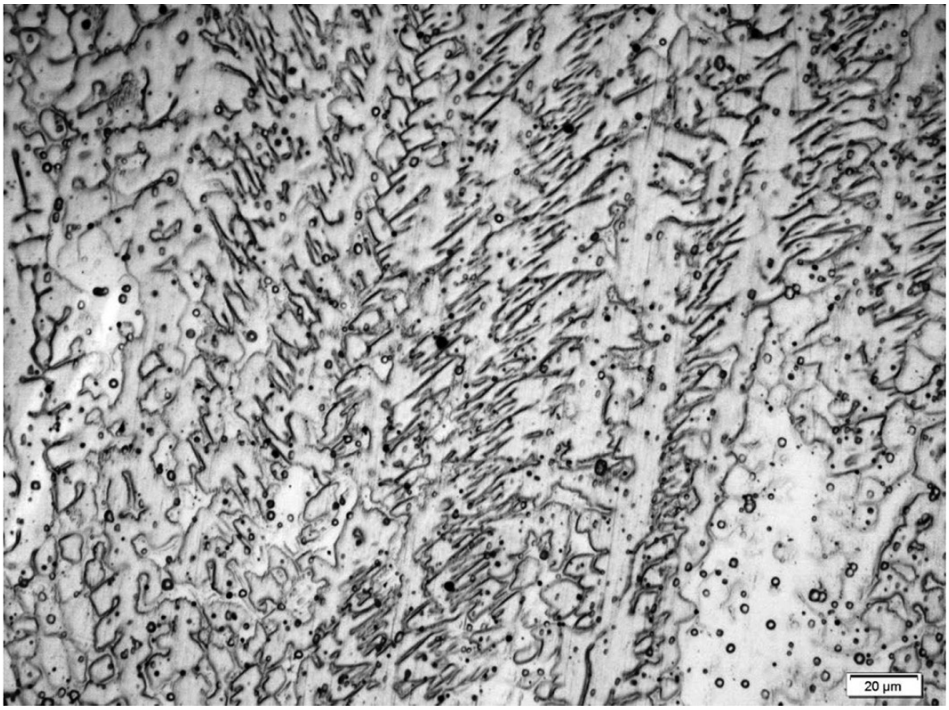

Figure 3—Weld metal microstructure of electrode C. Original magnification 500×

weld metal from electrode C contained fewer inclusions, there were larger particles relative to the weld metal from the other two electrodes, which had very similar particle size distributions. For electrodes A and B, the distribution of inclusion size peaked at 1 µm; for electrode C, the peak inclusion size was 3.5 µm. The total inclusion content for electrode C was lower, but this weld metal contained, on average, larger inclusions.

Linear regressions of the impact energy and lateral expansion results were carried out with respect to FN, the inclusion content, and temperature as variables, as given by Equation [2]:

$$X = A + A_1(\text{inclusion content}) + A_3(\text{FN}) + A_3(\text{temperature}) \quad [2]$$

where X is either the lateral expansion (mm) or impact energy (J), A is the intercept, and A_1 to A_3 are the coefficients of the indicated variables. The results are set out in Table V. Correlation coefficient R^2 values of 0.85 and 0.86 were obtained for the linear regressions of the impact energy and lateral expansion, respectively.

Discussion

The results showed that the weld metal produced with electrode C had fewer inclusions and higher impact toughness at all temperatures than those of electrodes A and B. As stated, the flux basicity of this electrode was 0.32. The weld metal of electrode C had an inclusion content of 1.4%, compared with electrodes A and B with basicities of 0.31 and 0.30 which resulted in an inclusion content of about 3.78% and 3.74% , respectively. Because the flux basicities were so similar, it could not be assessed, based on this result, whether the basicity affected the inclusion content. For electrode B, the high inclusion content may be associated with the high Si content in the weld metal, as a higher Si content in the weld metal may be the result of less deoxidation of the weld metal. For the same reason, the lower weld metal Si content and the low inclusion content of electrode C may be associated. The chemical composition of individual inclusions was not determined; such work presents a useful avenue for further study. The chemical composition of inclusions may help to explain the differences in the inclusion size that could not be explained using the current results. The large number of inclusions visible on the fracture surfaces of the scanning electron micrographs supports the hypothesis that the inclusion content affects impact toughness. Broken inclusions were particularly prominent in the fracture surface of weld metal from Electrode A, which consistently exhibited the lowest impact toughness (Figure 1). The most likely explanation of this effect is that an inclusion acts as an initiation site for micro-void decohesion, as evidenced by the enlarged 'cup'-type structures surrounding broken inclusions (Figure 4a). This indicates that an increase in inclusion content will decrease the energy required to fracture the steel and is supported by the impact results of electrodes A and B (Table IV and Figure 1), which clearly indicate that an increase in the inclusion content decreased the impact toughness of the weld metal. From Table IV, for one percentage of inclusions added to the weld metal, the impact toughness should decrease by 8.54 J. For the same increase in inclusion content, the lateral expansion should decrease by 0.091 mm. The statistical significance of these results is quantified by the P-values for the effect of inclusion content on the impact toughness (0.00036) and on the lateral expansion (0.02). A P-value below 0.05 is deemed to indicate a statistically significant effect. In contrast, the P-value for the effect of δ-ferrite content (quantified with FN) on the lateral expansion was 0.98, indicating that the FN had no statistically significant effect on the lateral expansion. The P-value for the effect of FN on the impact energy was 0.042, only marginally below 0.05.

In contrast to results of previous work, the high FN of the weld metal from electrode C did not result in a significant reduction in impact toughness at lower temperatures; this was one of the surprising observations of this study. The observation that, at low testing temperatures, any δ-ferrite in the weld metal will

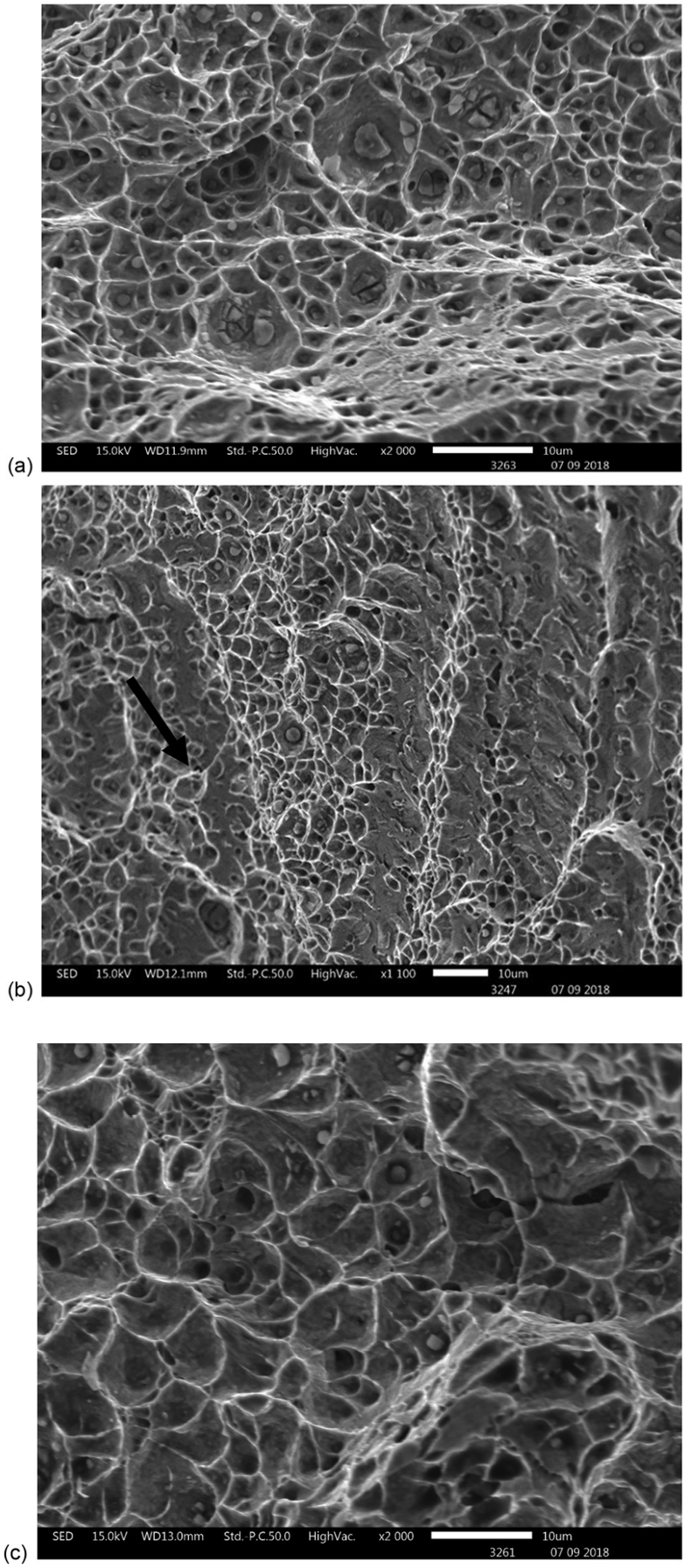

Figure 4—Fracture surfaces of weld metal Charpy impact specimens tested at –196°C, showing fracture inclusions. (a) Electrode A (measured impact toughness: 32 J); (b) electrode B (measured impact toughness: 46 J); (c) electrode C (measured impact toughness 46 J)

Table V

Linear regression results

Coefficient	Lateral expansion			Impact energy		
	Value	Standard error	P value	Value	Standard error	P-value
A (intercept)	1.52	0.12	7.01×10^{-11}	95.3	6.56	9.85×10^{-12}
A_1 (inclusion content)	-0.091	0.035	0.02	−8.54	1.97	0.00036
A_2 (FN)	0.00038	0.019	0.98	2.31	1.06	0.042
A_3 (temperature)	0.0043	0.00042	3.42×10^{-9}	0.23	0.02	1.08×10^{-8}

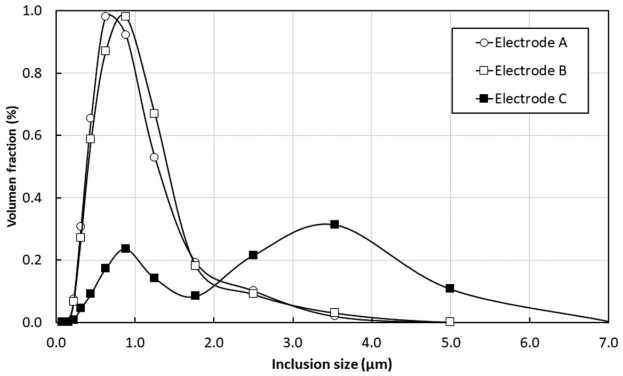

Figure 5—Inclusion size distributions in weld metal

result in a reduction in impact toughness (Lee and Dew-Hughes, 1982) may provide an explanation for the high impact toughness of weld metal from electrode C at low temperatures. All three weld metals contained significant amounts of δ-ferrite (as quantified in terms of the FN), and differences in impact toughness for the three weld metals evaluated in this study were primarily related to the inclusion content.

Conclusions

Three electrodes were examined to determine whether the composition of a shielded-metal arc-welding electrode coating affected the low-temperature impact toughness of austenitic stainless steel weld metal. The following conclusions were drawn from the results.

- The electrode coatings of electrodes A, B, and C were all acidic and showed very little difference in chemical composition or basicity.
- The weld metal from electrode C, which had a lower inclusion content (1.4%), had a higher impact toughness at all temperatures than the weld metals deposited from electrodes A and B, which had inclusion contents of about 3.8%.
- The impact energy was, as expected, sensitive to the inclusion content and testing temperature. That an increase in the amount of δ-ferrite resulted in slightly higher impact toughness was unexpected.
- The ferrite content had no statistically significant effect on lateral expansion. Linear expansion was sensitive to the testing temperature and inclusion content.
- The nitrogen content, in the range encountered in this study, did not affect the impact toughness or lateral expansion.

Acknowledgements

The support of the Southern African Institute of Welding and Columbus Stainless is gratefully acknowledged.

References

AWS SFA-5.4/SFA-5.4M:2006. Specification for stainless steel electrodes for shielded metal arc welding. American Welding Society, Miami, FL.

Entrekin Jr, C.H. 1979. The influence of flux basicity on weld-metal microstructure. *Metallography*, vol. 12, no. 4. pp. 295–312.

Hertzberg, R.W. 1995. Transition temperature approach to fracture control. *Deformation and Fracture Mechanics of Engineering Materials*. Wiley Hoboken, NJ. pp. 375–401.

Kamiya, O., Kumagai, K., and Kikuchi, Y. 1992. Effects of delta ferrite morphology on low-temperature fracture toughness of austenitic stainless steel. *Quarterly Journal of the Japan Welding Society*, vol. 9, no. 4. pp. 525–531.

Kotecki, D.J. and Siewert, T.A. 1992. WRC-1992 constitution diagram for stainless steel weld metals: a modification of the WRC-1988 diagram. *Welding Journal*, vol. 71, no. 5. pp. 171–178.

Lee, K. and Dew-Hughes, D. 1982. The effect of delta-ferrite upon the low temperature mechanical properties of centrifugally cast stainless steels. *Austenitic Steels at Low Temperatures*. Horiuchi, T. and Reed, R.P. (eds). Springer Science & Business Media. pp. 221–242.

Linnert, G.E. 1994. Transfer of elements between SAW flux/slag and weld metal. *Welding Metallurgy, Carbon and Alloy Steels*, vol. 1. American Welding Society. pp. 759–761.

Lippold, J.C. and Kotecki, D.J. 2005. *Welding Metallurgy and Weldability of Stainless Steels*. Wiley Hoboken, NJ.

Read, D.T., McHenry, H.I., Steinmeyer, P., and Thomas Jr, R.D. 1980. Metallurgical factors affecting the toughness of 316 L SMA weldments at cryogenic temperatures. *Welding Journal*, vol. 59, no. 4. pp. 104s–113s.

Reed, R. and Horiuchi, T. 1982. *Austenitic Stainless Steel at Low Temperatures*. Plenum Press, New York.

Saxena, A., Kumaraswamy, A., Reddy, G., and Madhu, V. 2018. Influence of welding consumables on tensile and impact properties of multi-pass SMAW Armox 500T steel joints vis-a-vis base metal. *Defence Technology*, vol. 14, no. 3. pp. 188–195.

Szumachowski, E. and Reid, H. 1978. Cryogenic toughness of SMA austenitic stainless steel weld metals: Part l - Role of ferrite. *Welding Journal*, vol. 57, no. 11. pp. 325s–333s.

Szumachowski, E. and Reid, H. 1979. Cryogenic toughness of SMA austenitic stainless steel weld metals: Part ll - Role of nitrogen. *Welding Journal*, vol. 58, no. 2. pp. 34s–44s. ◆